Co-Simulation of Electrical Networks by Interfacing EMT and Dynamic-Phasor Simulators

K. Mudunkotuwa, S. Filizadeh

***Abstract*--The paper presents a hybrid co-simulator comprising EMT and dynamic phasor-based simulators. The EMT simulator models part(s) of the network wherein fast transients are prevalent and detailed modeling is necessary. The dynamic phasor solver models the rest of the network using extended-frequency Fourier components. Specialized algorithms are developed and presented to accurately map instantaneous EMT and counterpart dynamic phasor samples. The paper demonstrates the developed co-simulator using an example of the IEEE 118-bus three-phase network in which a wind farm is included. The wind farm and the network in its vicinity are modeled in the PSCAD/EMTDC electromagnetic transient simulator, and are interfaced to the rest of the system modeled in a dynamic phasor-based solver. The paper demonstrates the accuracy of the proposed co-simulation for a range of time-step ratios of the two solvers, and also reports the substantial computational time savings obtained using the hybrid simulator.**

***Keywords*: Co-simulation, electromagnetic transient simulation, dynamic phasors, interfacing.**

I. INTRODUCTION

ELECTROMAGNETIC transient (EMT) simulation of large electrical networks is a challenging task due to the inherent computational intensity of EMT models and solution methods. EMT simulation of fast transients, e.g., switching events of high-power electronic converters, is particularly cumbersome as it needs small simulation time-steps to accurately capture high-frequency components. Under such circumstances, the entire network will be simulated with a small time-step, even though fast transients may only be confined to small portions thereof. With the proliferation of switching converters in modern power systems, it is increasingly necessary to use EMT simulations for larger systems to the extent that the required computational resources have nearly always outpaced the computing power of contemporary computers.

Several methods have been proposed to extend the applicability of EMT simulators in the study of large and complex power systems. Simplifications to individual component models, which is widely applied to high-frequency power electronic converters and is referred to as averaging, is one such method [1,2]. Alternatively, dynamic equivalents represent a portion of a large network by aggregating several components in a reduced-order model to relieve the computational intensity of simulation of the whole network [3-5]. Dynamic equivalents often yield significant reduction in the number of nodes to be included in the system's equivalent admittance matrix. In both the averaged-value and dynamic equivalent modeling approaches, a single EMT simulator will solve the entire network containing regular EMT-type and averaged or dynamic equivalent models.

Co-simulation is another approach to enable EMT-type simulation of a large network. Co-simulation is based upon an interface established between an EMT simulator and another solver. The two simulators will each solve a portion of the network under consideration concurrently. Since constituent simulators may not necessarily simulate networks in the same domain (i.e., time or frequency), simulated waveform samples need to be properly transferred from one simulator to another; this requires specific mapping algorithms. Examples of co-simulation have been reported by interfacing EMT simulation with transient-stability programs [6-8], finite-element simulation [9], and software- and processor-in-loop simulation [10,11]. Real-time EMT simulation with control and power hardware-in-loop interfaces are reported and reviewed in [12].

This paper proposes a co-simulation environment by interfacing an EMT simulator with an extended-frequency dynamic phasor-based solver. Previous studies have mentioned and partially shown the benefits of a hybrid EMT and dynamic phasor simulator [13,14]; however, the work presented herein is the first such co-simulator with numerical stability, and the ability to include a wide range of harmonics. The EMT simulator is used to simulate parts of the network where fast transients are present, e.g., in the electrical vicinity of fast-acting controllers and switching power-electronic converters. Such portions of the network require detailed modeling and small simulation time-steps. The dynamic-phasor solver represents the rest of the network, where fast transients are less pronounced or their representation is not necessary and can be avoided for computational gains. Segmentation of a large network into EMT and dynamic-phasor portions enables use of simulation algorithms that are best suited for each individual portion without having to incur either large computational burdens or large inaccuracies.

Following a detailed description of the established interface, an algorithm is proposed to provide mapping between EMT and dynamic phasor samples across the interface. The efficacy of the proposed interface is demonstrated via co-simulation of the IEEE 118-bus system

This work was supported in part by the University of Manitoba, and in part by the Natural Sciences and Engineering Research Council (NSERC) of Canada.
K. Mudunkotuwa is with Manitoba HVDC Research Center, Winnipeg, MB, Canada R3P 1A3, (email: ckumara@hvdc.ca).
S. Filizadeh is with the Department of Electrical and Computer Engineering, University of Manitoba, Winnipeg, MB, R3T 5V6, Canada, (e-mail of corresponding author: shaahin.filizadeh@umanitoba.ca).

Paper submitted to the International Conference on Power Systems Transients (IPST2017) in Seoul, Republic of Korea June 26-29, 2017

wherein a wind farm is embedded.

II. Mathematical Principles of Dynamic Phasors

A dynamic phasor is a harmonic component of the Fourier spectrum of a waveform. Consider a real-valued waveform $x(\cdot)$ over the interval $(t-T,T]$. The length of the interval T may be selected arbitrarily, although in the study of power-electronic converters it is normally chosen to be the converter's switching period [15]. The waveform $x(\cdot)$ is represented over the considered interval using the following Fourier series:

$$x(t-T+s)=\sum_{h=-\infty}^{+\infty}\langle x\rangle_h(t)e^{jh\frac{2\pi}{T}(t-T+s)} \quad s\in(0,T] \tag{1}$$

where $\langle x\rangle_h(t)$ is the Fourier coefficient corresponding to the h-th harmonic; $\langle x\rangle_h(t)$ is shown as an explicit function of time to stress the fact that the waveform's harmonics may change over time as the sliding window moves along the time axis. These Fourier coefficients are determined using conventional Fourier formulation shown below.

$$\begin{aligned}\langle x\rangle_h(t)&=\frac{1}{T}\int_0^T x(t-T+s)e^{-jh\frac{2\pi}{T}(t-T+s)}ds\\ \langle x\rangle_{-h}(t)&=\left(\langle x\rangle_h(t)\right)^*\end{aligned} \tag{2}$$

where * denotes complex conjugate.

It is straightforward to note that (1) can be re-written as an explicitly real-valued infinite series as follows.

$$x(t-T+s)=\langle x\rangle_0(t)+2\,\mathrm{Re}\left(\sum_{h=1}^{+\infty}\langle x\rangle_k(t)e^{jh\frac{2\pi}{T}(t-T+s)}\right) \tag{3}$$

Therefore, it is noted that the dynamic phasor corresponding to the h-th harmonic component is $2\langle x\rangle_h(t)$, which denotes the time-varying magnitude and phase of a harmonic that has an angular frequency of $h\frac{2\pi}{T}$.

Basic circuit components (i.e., resistors, inductors, and capacitors) can be readily expressed using extended-frequency dynamic phasors by applying the above formulae to their characteristic time-domain equations as shown in [16]. Once obtained, elements' characteristic equations can be discretized using a suitable integration method (e.g., the trapezoidal method) for discrete-time simulations on a digital computer.

Other circuit components, such as machines and converters, may also be similarly modeled using dynamic phasors [17, 18] and connected to the rest of the network as dynamic current-injecting sources similar to a conventional EMT solver, which is based upon an admittance matric formulation.

It is important to note that the formulations in (1) and (3) are based upon individual harmonic components (denoted by h); alternatively, one can re-formulate (3) into an equivalent form shown in (4), which effectively represents all harmonic components as a single harmonic component at the base angular frequency of $\frac{2\pi}{T}$.

$$x(t-T+s)=\ldots$$
$$\mathrm{Re}\left(\left(\begin{aligned}&\langle x\rangle_0(t)e^{-j\frac{2\pi}{T}(t-T+s)}+\ldots\\ &2\sum_{h=1}^{+\infty}\langle x\rangle_h(t)e^{j(h-1)\frac{2\pi}{T}(t-T+s)}\end{aligned}\right)e^{j\frac{2\pi}{T}(t-T+s)}\right) \tag{4}$$

Using (4) one can define a base-frequency dynamic phasor involving all harmonic components (including dc) as follows.

$$\mathbf{X}(t)=\langle x\rangle_0(t)e^{-j\frac{2\pi}{T}(t-T+s)}+2\sum_{k=1}^{+\infty}\langle x\rangle_h(t)e^{j(h-1)\frac{2\pi}{T}(t-T+s)} \tag{5}$$

It is straightforward to see that a reasonable approximation of a waveform can be obtained by considering only a subset of constituent harmonics in its Fourier expansion in (1) [15]. For example, 0-th (h = 0) and 1-st (h = 1) components may be considered adequate to represent dc and ac quantities in a power-electronic converter, respectively. Additional accuracy is obtained merely by including higher frequency components, thus the notion of extended-frequency dynamic phasors [16]. This observation can be readily extended to (5) as well. In other words, one may include only a small subset or as many harmonic components as desired in (5) to represent the base-frequency composite dynamic phasor of a waveform. Naturally, inclusion of a larger number of harmonics will yield a more accurate representation of a waveform.

Full harmonic preservation is adopted in the following section where an interface between a dynamic-phasor solver and an EMT solver (hereinafter called a DP-EMT simulator) is described. In other words, all dynamic phasor quantities in the following sections are similar to (5) and include the entire simulated harmonic spectrum; note that they are at the fundamental frequency although they are augmented with full harmonic (and dc) components as denoted in (5).

III. DP-EMT Interface: Layout and Algorithm

A. Interface layout

The functional form of the established DP-EMT interface is a transmission line with EMT and dynamic-phasor quantities at its two ends. EMT-type programs conventionally use traveling wave models to represent transmission lines. Travelling wave models introduce natural decoupling to the nodal equations of an EMT simulator [19]. More specifically, the two networks at the sending and receiving ends of a transmission line are isolated due to the line's finite travel-time or transportation-time delay, also known as transmission line latency. Fig. 1 shows the equivalent impedance representation of the Bergeron lossless line model. This model is used to establish an interface between EMT and dynamic phasor solvers.

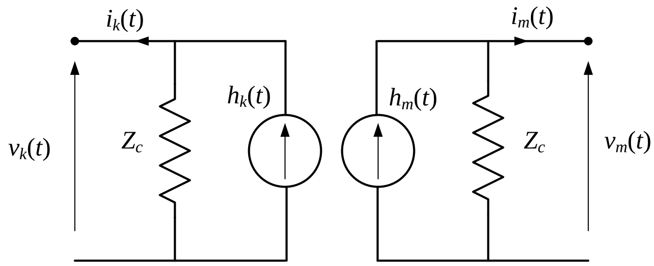

Fig. 1. A lossless transmission line segment model.

Current-source injections at the two ends are as follows.

$$h_k(t) = \frac{2v_m(t-\tau)}{Z_c} - h_m(t-\tau) \tag{6}$$

$$h_m(t) = \frac{2v_k(t-\tau)}{Z_c} - h_k(t-\tau) \tag{7}$$

where τ is the travel-time delay, and Z_c is the line's characteristic impedance. According to (6) and (7), current injections at nodes k and m at time t are calculated using quantities at the other node at time t-τ. This natural latency allows that the two sides of the line to be simulated using different modeling approaches such EMT and dynamic phasor solvers.

Consider a situation where the nodes k and m represent the dynamic-phasor and EMT network segments, respectively. The equivalent impedance model of such a DP-EMT model is similar to Fig. 1; however, the corresponding quantities on the node-k side are dynamic phasors and quantities on the node-m side are EMT samples.

The DP form of (6) is as follows:

$$H_k(t) = \left[\frac{2V_m(t-\tau)}{Z_c} - H_m(t-\tau)\right] e^{-j\tau\omega} \tag{8}$$

According to (8), in order to calculate the current injection at node k, instantaneous quantities at the EMT side (i.e., $v_m(t-\tau)$ and $h_m(t-\tau)$) are needed be converted to the equivalent DP quantities. Similarly, to determine the current injection at node m using (7), the DP quantities at node k need to be converted to instantaneous quantities. Therefore, bi-directional signal conversion is required to realize the proposed DP-EMT hybrid transmission line.

B. Sample conversion (DP to EMT and EMT to DP)

Conversion of a dynamic phasor $\mathbf{X}(t)$ to time-domain is simply done using the following formula.

$$x(t) = \mathrm{Re}\left(\mathbf{X}(t) e^{j\frac{2\pi}{T}t}\right) \tag{9}$$

Conversion of EMT simulation samples, however, is more challenging. Note that (5) shows how a fully-augmented dynamic phasor at the base frequency can be obtained. It is, however, noted that calculation of $\mathbf{X}(t)$ using (5) requires all individual Fourier components, $\langle x \rangle_h(t)$, to be available. Although calculation of these components is possible using (2), it is not desirable to do so as it entails numerical integration for each component and hence a large computational burden. Alternatively, it is noted that the following equality holds.

$$x(t-T+s) = \underbrace{2\,\mathrm{Re}\left(\langle x \rangle_1(t) e^{j\frac{2\pi}{T}(t-T+s)}\right)}_{\text{fundamental component}} + \ldots$$
$$\underbrace{\left(\sum_{\substack{h=-\infty \\ h\neq -1,1}}^{+\infty} \langle x \rangle_h(t) e^{-j(h-1)\frac{2\pi}{T}(t-T+s)}\right) e^{j\frac{2\pi}{T}(t-T+s)}}_{\text{dc + harmonics}} \tag{10}$$

Therefore, if $\langle x \rangle_1(t)$ is calculated using (2), then the first term on the right-hand side of (10) can be calculated and then subtracted from the already available left-hand side. Doing so yields the second term on the right-hand side of (10), which includes all dc and harmonic contents of the EMT waveform, from which the corresponding fully-augmented fundamental-frequency dynamic phasor can be readily calculated as per (5). This method circumvents direct calculation of (5) using individual harmonic components and yields the same fully augmented fundamental-frequency dynamic phasor with much reduced complexity.

In the following section, a case study of co-simulation using the developed DP-EMT interface is shown. The example demonstrates the accuracy and computational advantages of the proposed co-simulation method.

IV. Co-Simulation Example Case

The IEEE 118-bus test system [20] is used to illustrate the accuracy and efficacy of the proposed DP-EMT co-simulator. As shown schematically in Fig. 2 a small portion (3 buses) of the system containing a Type-4 wind farm of 75 turbines (6 MW each) [21] is modeled in an EMT simulator (PSCAD/EMTDC) including detailed switching-level models of power electronic converters. An aggregate representation is used to model the wind farm, where only one wind turbine is simulated and is then scaled up to represent the concurrent operation of several wind turbines in the farm. The total capacity of the wind farm is 450 MW.

The remaining 115 buses of the system are modeled in the dynamic phasor domain in a custom simulation environment and the proposed DP-EMT interface is used to connect the two simulators. The existing 150-km transmission line between buses 9 and 8 is used as the DP-EMT interface. The positive sequence parameters of this line are shown in Table 1. Communication between the two simulators is established using the control network interface (TCP/IP-based) of PSCAD/EMTDC.

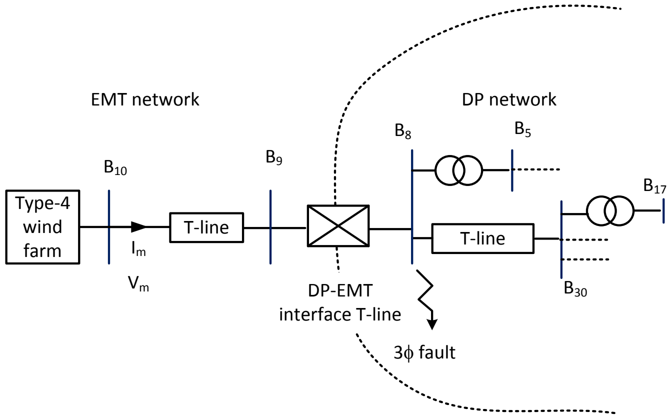

Fig. 2. Segmented IEE118-bus test system with a wind farm.

TABLE I TRANSMISSION LINE (B_8 TO B_9) PARAMETERS (POSITIVE SEQUENCE)

Parameter	Value [pu] on a 138kV/100 MVA base
R (series resistance)	0.0025
X (series reactance)	0.0305
B (shunt admittance)	1.1620

Three sets of simulations are conducted: (1) a DP-EMT co-simulation with a 20-μs time step in both simulators; (2) a DP-EMT co-simulation with 500-μs and 20-μs time-steps for the DP and EMT segments, respectively; and (3) a full EMT simulation with a 20-μs time step. The full EMT simulation is used to validate the results of the DP-EMT co-simulations.

The first co-simulation with equal 20-μs time-steps for both simulators is meant to verify that the co-simulator is able to replicate full EMT results. The second co-simulation with a 25:1 time-step ratio is meant to show that significant acceleration will be achieved with the use of a larger time step for the dynamic phasor segment while maintaining the accuracy of representation of low-frequency oscillations.

In all simulations, a three-phase-to-ground fault is applied at bus 8 (see Fig. 2) at t = 1.8 s and cleared 6 cycles later. Current and voltage measurements are captured at bus 10 (within the EMT segment) and bus 30 (within the DP segment).

Fig. 3 shows a comparison between the results of the hybrid DP-EMT (20-μs:20-μs) co-simulation and the fully detailed EMT model of the whole network. These plots show that the DP-EMT simulator has complete conformity with the full EMT simulator when equal time-steps are used. This is due to the fact that fully-augmented fundamental-component dynamic phasors of EMT waveforms at the interface boundary are calculated and transferred to the dynamic phasor segment, thereby preserving the entire simulated harmonic spectrum.

Fig. 4 shows a comparison between the results of the hybrid DP-EMT (500-μs:20-μs) and the fully detailed EMT model of the whole network. These plots show that the DP-EMT simulator is able to capture the low-frequency contents of the waveforms before, during, and after the fault; some high-frequency transients are not observed in the DP-EMT results due to the fact that use of a larger time-step to gain simulation speed results in less harmonic bandwidth in the simulated waveforms.

Fig. 5 shows a comparison of the per-unit (positive sequence, fundamental frequency only) rms voltage as well as real and reactive power at the wind farm terminal for the DP-EMT (500-μs:20-μs) co-simulation. These traces clearly show the DP-EMT co-simulator closely replicates the results obtained using the full EMT model of the whole network.

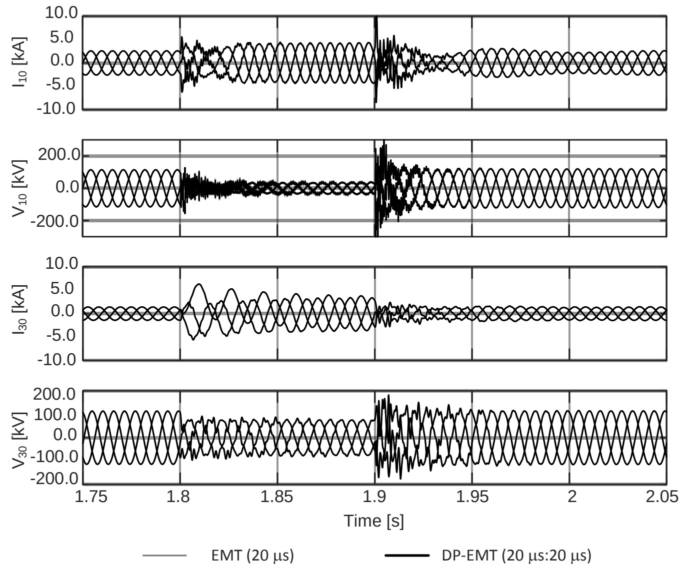

Fig. 3. Instantaneous current and voltage waveforms at bus 10 (top two plots) and bus 30 (bottom two plots) for EMT (20-μs) and DP-EMT (20-μs:20-μs) simulations.

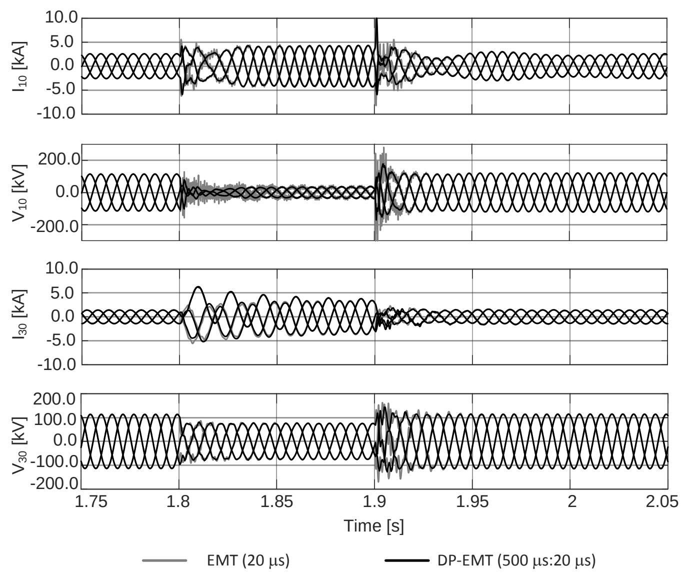

Fig. 4. Instantaneous current and voltage waveforms at bus 10 (top two plots) and bus 30 (bottom two plots) for EMT (20-μs) and DP-EMT (500-μs:20-μs) simulations.

Table II shows the simulation time comparison between the full EMT (the entire network at 20 μs) and the DP-EMT (500 μs:20 μs) simulations for a simulation duration of 3 s. As seen, the DP-EMT co-simulation is more than 5 times faster than the EMT solver, thereby offering significant computational relief. This reduction in simulation time is while maintaining the accuracy of simulated results in terms of low-frequency dynamics, as is shown in Figs. 4 and 5.

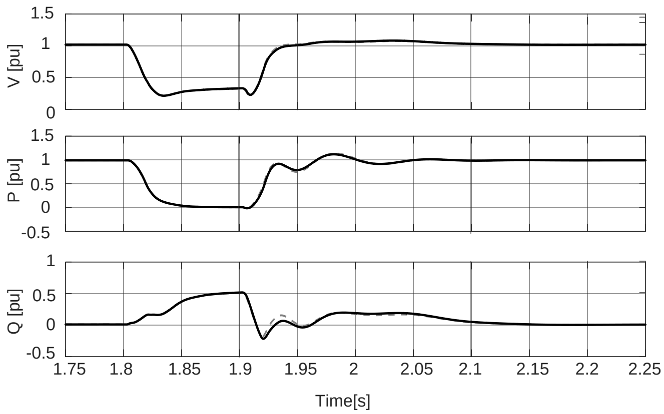

Fig. 5. Terminal voltage (rms, fund.), and real and reactive power at the wind farm terminal for EMT (20-μs) and DP-EMT (500-μs:20-μs) simulations.

It must be noted that the speed-up gain is due to the reduction of the number of floating point operations required to simulate the external subsystem (i.e., the DP side). The overall speed is still heavily influenced by the EMT side, where detailed representation of switching events in the wind farm converters consumes considerable time. In fact, replacement of the wind farm in this network with a controlled and dynamically-adjusted voltage source resulted in a speed-gain of more than 22, which is due the simplified switching converter model (simulation traces are not shown for brevity).

TABLE II SIMULATION TIME COMPARISON

Simulator	Time taken for a 3-s simulation
EMT for the whole network	694 s
DP-EMT	132 s
DP-EMT(voltage source)	32 s

V. CONCLUSIONS

The paper proposed and implemented an interface between an EMT and a dynamic-phasor solver for co-simulation of electrical networks. The rationale for such a co-simulator is to enable and expedite simulation of large electrical networks wherein fast-acting controllers and switching power-electronic converters are embedded. By taking advantage of the harmonic selectivity of dynamic phasor-based modeling, the proposed co-simulator offers significant computational relief compared with an EMT simulator.

The paper described how simulated samples are converted from the EMT domain to dynamic phasors and vice versa, and transmitted across the transmission line interface. In particular, a computationally efficient method was described for conversion of EMT samples to dynamic phasors, which retained the full harmonic spectrum of the EMT waveform and represented it as a dynamic phasor at fundamental frequency.

The paper also showed co-simulation results of a representative network in which a large wind farm was embedded. It was shown that depending on the simulation time-steps used, the developed DP-EMT co-simulator is able to capture both the low- and the high-frequency contents of waveforms in both the EMT and dynamic phasor segments of the network, and offer significant computational relief; a speed gain of larger than 5 was obtained in the shown example.

VI. REFERENCES

[1] S. Chiniforoosh, J. Jatskevich, A. Yazdani, V. Sood, V. Dinavahi, J. A. Martinez, and A. Ramirez, "Definitions and Applications of Dynamic Average Models for Analysis of Power Systems," *IEEE Transactions on Power Delivery*, vol. 25, no. 4, pp. 2655-2669, Oct. 2010.

[2] H. Ouquelle, L. A. Dessaint, and S. Casoria, "An Average Value Model-Based Design of a Deadbeat Controller for VSC-HVDC Transmission Link," in *Proc. 2009 IEEE Power & Energy Society General Meeting*, pp. 1-6.

[3] S. E. M. de Oliveira, and A. G. Massaud, “Modal Dynamic Equivalent for Electric Power Systems I: Theory,” *IEEE Trans. Power Syst*., vol. 3, no. 4, pp. 1731–1737, Nov. 1988.

[4] U. D. Annakkage, N. K. C. Nair, Y. Liang, A. M. Gole, V. Dinavahi, B. Gustavsen, T. Noda, H. Ghasemi, A. Monti, M. Matar, R. Iravani, and J. A. Martinez, "Dynamic System Equivalents: A Survey of Available Techniques," *IEEE Transactions on Power Delivery*, vol. 27, no. 1, pp. 411-420, Jan. 2012.

[5] F. Ma, and V. Vittal, "Right-Sized Power System Dynamic Equivalents for Power System Operation," *IEEE Transactions on Power Systems*, vol. 26, no. 4, pp. 1998-2005, Nov. 2011.

[6] J. M. Zavahir, J. Arrillaga, and N. R. Watson, "Hybrid Electromagnetic Transient Simulation with the State Variable Representation of HVDC Converter Plant," *IEEE Trans. Power Delivery*, vol. 8, no. 3, pp. 1591–1598, July 1993.

[7] V. J. Marandi, V. Dinavahi, K. Strunz, J. A. Martinez, and A. Ramirez, “Interfacing Techniques for Transient Stability and Electromagnetic Transient Programs,” *IEEE Trans. Power Delivery*, vol. 24, no. 4, pp. 2385-2395, Oct. 2009.

[8] X. Wang, P. Zhang, Z. Wang, V. Dinavahi, G. Chang, J. A. Martinez, A. Davoudi, A. Mehrizi-Sani, and S. Abhyankar, “Interfacing Issues in Multiagent Simulation for Smart Grid Applications,” *IEEE Trans. Power Delivery*, vol. 28, no. 3, pp. 1918-1927, July 2013

[9] B. Asghari, V. Dinavahi, M. Rioual, J. A. Martinez, and R. Iravani, “Interfacing Techniques for Electromagnetic Field and Circuit Simulation Programs,” *IEEE Trans. Power Delivery*, vol. 24, no. 2, pp. 939-950, April 2009.

[10] H. Vardhan, B. Akin, and H. Jin, “A Low-Cost, High-Fidelity Processor-in-the-Loop Platform,” *IEEE Power Electronics Magazine*, vol. 3, no. 2, pp. 18-28, June 2016.

[11] G. Chongva, S. Filizadeh, “Non-Real-Time Hardware-in-Loop Electromagnetic Transient Simulation of Microcontroller-Based Power Electronic Control Systems,” in *Proc. 2013 IEEE Power Engineering Society General Meeting*, pp 1-5.

[12] W. Ren, M. Sloderbeck, V. Dinavahi, S. Filizadeh, A. R. Chevrefils, M. Matar, R. Iravani, C. Dufour, J. Belanger, M. O. Faruque, K. Strunz, and J. A. Martinez, “Interfacing Issues in Real-Time Digital Simulators,” *IEEE Trans. on Power Delivery*, vol. 26, no. 2, pp.1221-1230, April 2011.

[13] F. Plumier: ‘Co-simulation of Electromagnetic Transients and Phasor Models of Electric Power Systems’. Ph.D. Dissertation, University of Liège, 2015.

[14] K. M. H. K. Konara: ‘Interfacing Dynamic Phasor Based System Equivalents to an Electromagnetic Transient Simulation’. M.Sc. Thesis, University of Manitoba, 2014.

[15] S. R. Sanders, J. M. Noworolski, X. Z. Liu, and G. C. Verghese, “Generalized Averaging Method for Power Conversion Circuits,” *IEEE Trans. Power Elec*., vol. 6, no. 2, pp. 251-259, April 1991.

[16] M. A. Kulasza: ‘Generalized Dynamic Phasor-Based Simulation for Power Systems’. M.Sc. Thesis, Dept. of Elec. and Comp. Engineering University of Manitoba, 2014.

[17] S. Henschel, “Analysis of Electromagnetic and Electromechanical Power System Transient with Dynamic phasors,” Ph.D. dissertation, University of British Colombia, 1999.

[18] P. Zhang, J.R. Martí, H.W. Dommel, “Synchronous Machine Modeling Based on Shifted Frequency Analysis,” IEEE Trans. Power Systems, vol. 22. No. 3, pp.1139-1147. 2007.

[19] D. M. Falcao, E. Kaszkurewicz, and H. L. S. Almeida, “Application of Parallel Processing Techniques to the Simulation of Power System Electromagnetic Transients,” *IEEE Trans. Power Syst*., vol. 8, no. 1, pp. 90–96, Feb. 1993.

[20] IEEE 118-Bus System, Available: http://icseg.iti.illinois.edu/ieee-118-bus-system/

[21] *Wind Turbines—Part 27-1: Electrical Simulation Models—Wind Turbines*, IEC Standard 61400-27-1, ed. 1, Feb. 2015.